Available online at www.sciencedirect.com
ScienceDirect
Marine Pollution Bulletin 56 (2008) 677–685
MARINE POLLUTION BULLETIN
www.elsevier.com/locate/marpolbul

# Application of ultraviolet fluorometry and excitation–emission matrix spectroscopy (EEMS) to fingerprint oil and chemically dispersed oil in seawater

J.B.C. Bugden *, C.W. Yeung, P.E. Kepkay, K. Lee

*Centre for Offshore Oil and Gas Environmental Research (COOGER), Fisheries and Oceans Canada, Bedford Institute of Oceanography, 1 Challenger Drive, P.O. Box 1006, Dartmouth, NS, Canada B2Y 4A2*

**Abstract**

Excitation–emission matrix spectroscopy (EEMS) was used to characterize the ultra violet fluorescence fingerprints of eight crude oils (with a 14,470-fold range of dynamic viscosity) in seawater. When the chemical dispersant Corexit 9500® was mixed with the oils prior to their dispersion in seawater, the fingerprints of each oil changed primarily as an increase in fluorescence over an emission band centered on 445 nm. In order to simplify the wealth of information available in the excitation–emission matrix spectra (EEMs), two ratios were calculated. A 66–90% decrease in the slope ratio was observed with the addition of Corexit. When the slope ratios were reduced in complexity to intensity ratios, similar trends were apparent. As a result either of the ratios could be used as a simple and rapid means of identifying and monitoring chemically dispersed oil in the open ocean.


*Keywords:* Oil fluorescence; Oil fingerprints; EEMS; Dispersant; Emission ratios

## 1. Introduction

Oil can be released into the environment from a number of sources (National Research Council, 1985), and can cause serious ecological damage if not remediated. In order to implement a practical remediation strategy, the oil and corresponding by-products of remediation need to be identified and traced. Methods such as gas chromatography–flame ionization detection (GC–FID), gas chromatography–mass spectroscopy (GC–MS) and high-performance liquid chromatography (HPLC) are all sensitive tracer techniques, but require the extraction and concentration of samples prior to analysis. This means that a great deal of time is spent on the quantitative measurement and interpretation of the data (Muroski et al., 1996; Booksh et al., 1996; Jiji et al., 1999; Nahorniak and Booksh, 2003; Ryder et al., 2003; Ryder, 2004; Christensen et al., 2005). Any method that allows a more direct and rapid interpretive analysis of aquatic samples would be a useful addition to this battery of techniques.

Ultra-violet fluorescence spectroscopy (UVFS) has already been shown to be a rapid and sensitive way of obtaining information on the presence and relative concentration of many organic compounds in seawater (Østgaard and Jensen, 1983; Coble et al., 1990; Muroski et al., 1996; Booksh et al., 1996; Jiji et al., 1999; Nahorniak and Booksh, 2003; Christensen et al., 2005). As Patra and Mishra (2002) have pointed out, it is a particularly useful tool because it does not require the extraction and concentration procedures that are typical of other spectroscopic techniques like UV–visible, infrared (IR), Raman scattering and nuclear magnetic resonance (NMR). When applied to water samples (Coble, 1996, with references), UVFS has provided detailed information to identify natural dissolved organic matter (DOM). Fluorescence spectroscopy has also been utilized to estimate crude oil concentrations in natural waters (Keizer and Gordon, 1973; Østgaard and Jensen,

* Corresponding author. Tel.: +1 902 426 7256; fax: +1 902 426 1440.
*E-mail address:* BugdenJ@mar.dfo-mpo.gc.ca (J.B.C. Bugden).

0025-326X/$ - see front matter 
doi:10.1016/j.marpolbul.2007.12.022

1983). In addition, Kepkay et al. (2002) have used UVFS as a means of distinguishing between oil dispersed in seawater and the oil incorporated into oil–mineral aggregates (OMAs).

The fact that many organic compounds fluoresce at specific excitation and emission wavelengths is the basis for identifying many of the components of DOM and crude oil in seawater. For example, humic material fluoresces over emission wavelengths of 320–350 nm when subject to excitation at 230–260 nm, and proteins fluoresce over emission wavelengths of 300–350 nm with excitation at 220 and 275 nm (Coble, 1996, with references). In addition, when subject to excitation at 245–280 nm, polycyclic aromatic hydrocarbons (PAH) fluoresce over wavelengths of 310 to >400 nm, depending on the number of aromatic rings in the structure (Wakeman, 1977; Von der Dick and Kalkreuth, 1985; Biddleman et al., 1990; Patra and Mishra, 2002). The two-dimensional (2D) emission spectra of crude oils extracted into a variety of solvents (and subject to excitation at a single wavelength) generally resolve into a broad, featureless peak that extends over emission wavelengths of 310 to >400 nm (Biddleman et al., 1990; Nahorniak and Booksh, 2003; Christensen et al., 2005).

This lack of resolution inherent in the 2D UVFS of oils extracted into solvent has led to the application of excitation–emission matrix spectroscopy (EEMS), which can provide detailed three-dimensional (3D) information for the identification of fluorescent compounds in complex mixtures. EEMS has been used to characterize marine and terrestrial DOM and to identify its source (Coble et al., 1990; Coble, 1996, with references; Stedmon et al., 2003; Sierra et al., 2006). In addition, 3D fluorescence spectroscopy has been used to extract information from the constituents of crude oil and petroleum products (Von der Dick and Kalkreuth, 1985; Gugel and Siegel, 1988; Patra and Mishra, 2002; Hegazi et al., 2005; Muroski et al., 1996; Booksh et al., 1996; Babichenko et al., 1999; Jiji et al., 1999; Drozdowska and Babichenko, 2002; Nahorniak and Booksh, 2003; Christensen et al., 2005). Of particular interest is the utilization of EEMS to identify specific compounds in terms of their individual fluorescent fingerprint or signature. For example, Gugel and Siegel (1988) have used 3D spectra in forensic investigations to determine if petroleum-based products were from a similar source and Sikorska et al. (2004) have used the method to characterize beers. Von der Dick and Kalkreuth (1985) have also shown that 3D fluorescence can be used as a means of fingerprinting the maturation of coals and oils by detecting differences in the distribution of ring systems. Hegazi et al. (2005) have expanded on this approach, using remote sensing and time-resolved 3D fluorescence spectra to fingerprint crude oils, and as an extension of the earlier work, Babichenko et al. (1999) have employed a Fluo Imager linked to a library of reference spectra for organic compounds.

Even though much of the work with EEMS has been focussed on oils dissolved in solvents such as dichloromethane (Muroski et al., 1996; Booksh et al., 1996; Jiji et al., 1999; Nahorniak and Booksh, 2003; Christensen et al., 2005), there are some fingerprints available of oil dispersed in seawater (Babichenko et al., 1999). However, no one has looked at the alteration of fingerprints in response to natural weathering processes and/or treatments with chemical dispersants. The application of dispersants to oil slicks can lessen detrimental effects of the oil on the environment (Lessard and Demarco, 2000; Page et al., 2000), by facilitating the transport of oil into the water column in the form of small suspended droplets (Li and Garrett, 1998) which become dispersed by currents to concentrations below toxicity threshold limits. This retention of oil as small droplets with an enhanced surface to volume ratio in the water column makes them more accessible to natural hydrocarbon-degrading bacteria and thus promotes its removal from the environment (Lessard and Demarco, 2000; Venosa and Zhu, 2003, with references). As a result, we have used EEMS to determine the effect of Corexit 9500® in seawater on eight crude oils with a 14,470-fold range of dynamic viscosity. With information about slope ratios and maximum fluorescence intensity obtained from contour plots, we will show how EEMS can be used as a quick, reliable and cost-effective method to monitor the distribution of oil and chemically dispersed oil in the marine environment following an oil spill incident.

## 2. Methods

Eight reference crude oils from the Emergencies Science and Technology Division of Environment Canada were chosen to encompass a wide range of dynamic viscosity (Table 1) and be characterized in terms of their excitation–emission matrix spectra (EEMS). Five milliliters of oil were dispensed into 50 mL of 1-μm filtered seawater (at a nominal concentration of 100 ppm of oil) in a 90 mL specimen container (Fisher Scientific) using a Rainin LTS pipettor. In order to ensure that no oil remained in the pipet tip, the tip was rinsed three to five times with seawater, and each residue injected into the specimen cup. The oil/water sample was then placed on a reciprocal shaker (Eberbach Corp., Ann Arbor, Michigan) at approx-

Table 1
Dynamic viscosity (centipoise at 15 °C) of the eight oils evaluated

| Oil | Dynamic viscosity (DV) cP[1] |
|---|---|
| Scotian Light | 1 |
| Federated | 4 |
| Brent Blend | 6 |
| Gullfaks | 13 |
| Terra Nova | 22 |
| Hibernia | 49 |
| Maya | 280 |
| IFO 300 | 14,470 |

[1] Environment Canada, ETC Data base, 2001 (http://www.etc-cte.ec.gc.ca/databases/OilProperties/Default.aspx).

imately 280 oscillations per minute and shaken for 30 min to physically disperse the oil. Emulsions were not observed to form during the dispersion process.

To assess the influence of chemical oil–dispersants, 5 mL of oil was put into a 20 mL borosilicate scintillation vial (FisherBrand, Fisher Scientific) and 250 μL of dispersant (Corexit 9500®) was added to produce a 1:20 dispersant to oil ratio (DOR). This ratio was chosen based on the observation that one part dispersant will disperse about 20–30 parts of oil (Lessard and DeMarco, 2000), and falls within the range of 1:10 and 1:30 used by other researchers (Page et al., 2000; Yamada et al., 2003; Couillard et al., 2005). Even though the oil/dispersant mixture was vigorously shaken by hand for approximately 60 s prior to dispersion in 50 mL of seawater as described above, oil–water–dispersant emulsions were not observed to form. Duplicate runs for each oil and each oil–dispersant combination were also performed.

Three milliliters of the oil–water or oil–dispersant–water mix were transferred into a 4.5 mL UV-grade quartz cuvette (10 mm light path – Hellma (Canada) Limited, Concord, Ontario) using a Gilson P5000 Pipetman and Gilson D5000 5 mL tips. Ultraviolet (UV) fluorescence spectra were obtained with a RF-5301PC scanning spectrofluorometer (Shimadzu Corp., Kyoto, Japan) running Panorama fluorescence 1.1 software (LabCognition, Dortmund, Germany). To maintain homogenization, the sample was re-mixed between scans in the cuvette with a Gilson P1000 Pipetman and a Gilson P1000 pipet tip. In order to blank correct the spectra, scans of the 1-μm filtered seawater and seawater plus Corexit 9500® were obtained in the same manner as the oil–seawater and oil–dispersant–seawater samples. These blank spectra were then subtracted from the oil–seawater and oil–dispersant–seawater spectra, respectively, before EEMS contour plots were generated.

In order to generate excitation–emission matrix spectra (EEMs), several scans of emission wavelengths at fixed excitation wavelengths were collected and then combined. These were obtained by scanning the sample, adjusting the excitation and emission parameters (at the same time re-homogenizing the sample), and performing the next scan. Fourteen spectra were obtained beginning at 220 nm excitation, 240–485 nm emission and ending at 350 nm excitation, 370–615 nm emission. The step-increase of excitation between emission scans was 10 nm with a 20 nm separation between excitation and emission wavelengths. Slit widths of 10 nm excitation and 5 nm emission along with a sampling interval of 1.0 nm, a scan speed of approximately 8 nm/s, and the response time set to "auto" produced the best resolved spectra with the highest fluorescence intensities for all oils.

Contour plots of the EEMs were generated by exporting the data into Microsoft Excel spreadsheets (Microsoft Corp., Redmond, WA) to be plotted in Surfer 8 (Golden Software, Inc., Golden, Colorado). Prior to generation of the plots, the data were edited to remove the Raman peak detected at 220 and 230 nm excitation wavelengths and the Raman peak multiples observed at 240, 250, 260 and 270 nm excitation which effectively masked the fingerprints of the oils. Removal of the Raman peaks and multiples that dominated the spectra was carried out by excluding the data below 240 nm excitation, and deleting the values above 465 nm emission at 240 nm excitation, above 485 nm emission at 250 nm excitation, above 505 nm emission at 260 nm excitation, and above 525 nm emission at 270 nm excitation. Contour plots were generated as normalized blank-corrected data (where spectral intensity was converted to percent of maximum intensity) and as non-normalized blank corrected data only.

To aid in the interpretation of results, slope and intensity ratios were calculated from the contour plots of non-normalized data using the following expression:

$$\text{Slope ratio(SR)} = \frac{(I_{280\ \text{ex}} - I_{320\ \text{ex}})@340_{\text{em}}}{(I_{280\ \text{ex}} - I_{350\ \text{ex}})@445_{\text{em}}}$$

Intensity ratios were calculated using the formula:

$$\text{Intensity ratio } (\text{IR}_{280\ \text{ex}}) = \frac{I_{340}\ \text{em}}{I_{445}\ \text{em}}$$

## 3. Results

When the excitation–emission matrix spectra (EEMs) were expressed as normalized contour plots (Figs. 1 and 2), distinct differences among the eight test oils were apparent. Most obvious was that the oils of lower dynamic viscosity (Table 1) all showed a strong band of emission intensity between 400 and 500 nm (centered at about 445 nm) throughout the range of excitation wavelengths employed. The exception to this was the very low (1 cP) viscosity Scotian Light crude (Fig. 1A) where the band of maximum emission at 445 nm was much less intense and extended only to about 320 nm excitation. In addition, the 445 nm band was entirely absent in the higher viscosity oils, Maya and IFO 300 (Fig. 2C and D). Another band of maximum emission intensity was located at 340 nm (over an excitation range of 280–300 nm). This was visible in all of the crude oils (Figs. 1 and 2), but the shape and overall intensity of the 340 nm band varied considerably from oil to oil.

In general, when the oil was mixed with the chemical dispersant Corexit 9500® prior to dispersion in seawater, the overall intensity increased. For example, as illustrated in Fig. 3A and B, the effect of the dispersant on low viscosity oils (<50 cP) such as Brent Blend crude was an increase in intensity for both the 340 nm and the 445 nm emission bands. High viscosity oils, such as Maya and IFO 300 (the highest viscosity oil at 14,470 cP; Fig. 3C and D), also displayed a substantial increase in intensity at 445 nm relative to that observed for seawater and oil alone.

The locations of slope and intensity ratio calculations were established by choosing the maximum intensities within the two principal emission bands identified at 340

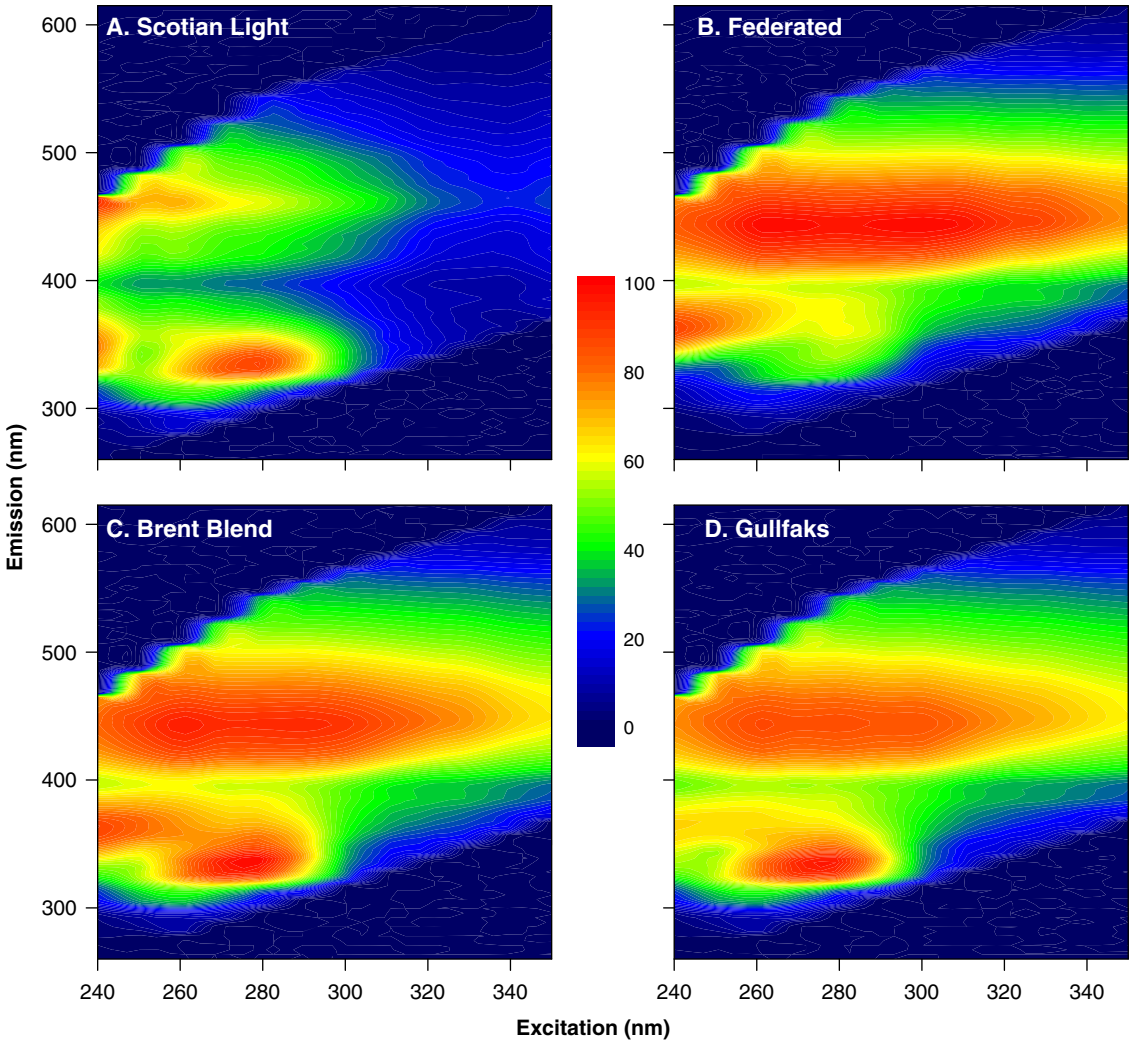


Fig. 1. Normalized intensity (reported as a percentage of maximum intensity) contour plots of excitation–emission matrix spectra (EEMs) of low viscosity (<50 cP) Scotian Light, Federated, Brent Blend, and Gullfaks crude oils.

and 445 nm. The results for the slope ratios of the eight oils are plotted against their dynamic viscosity in Fig. 4A. Oils with viscosities of <50 cP (Table 1) had slope ratios of <6 when dispersed in seawater (Table 2). In contrast, Maya crude and IFO 300 crude, with viscosities of 280 and 14,470 cP, had slope ratios of 20 and 45, respectively (Table 2). Addition of the dispersant lowered the slope ratio, but not in a uniform manner (Fig. 4). Oils with dynamic viscosities <50 cP exhibited reductions from an average of 4.5 to 1.5, or 66% (Table 2). In contrast (Fig. 4A and Table 2), the more viscous oils (with viscosities >50 cP) dropped by 86% (Maya) and 90% (IFO 300). Intensity ratios displayed the same trend (Fig. 4B); the addition of dispersant reduced the ratios of the six lower viscosity test oils by an average of 47%, compared to 77% for Maya crude and 84% for IFO 300 crude (Table 2). When the chemical composition of the oil (expressed as the percent by weight of aromatic compounds in the oil) was plotted against the intensity ratio (Fig. 4C), the same trend was also apparent.

## 4. Discussion

Our intent when applying excitation–emission matrix spectroscopy (EEMS) to crude oils dispersed in seawater was not only to determine the fingerprint of physically dispersed oil in seawater, but also to determine the influence of a chemical dispersant (Corexit 9500®) on the fingerprint. To facilitate comparison of treated and untreated oil samples, a numerical method was devised to simplify the analysis of complex 3D spectra.

### *4.1. Normalized contour plots and oil fingerprints*

Contour plots generated from the 3D excitation–emission matrix spectra (EEMs) of the eight test oils in seawater showed distinct differences, especially between low-viscosity oils (with dynamic viscosities, DVs <50 cP) and those with DVs >50 cP (Figs. 1 and 2). When the contour plots of the different oils were compared, variations in intensity obscured the subtle differences in the fingerprints. As a

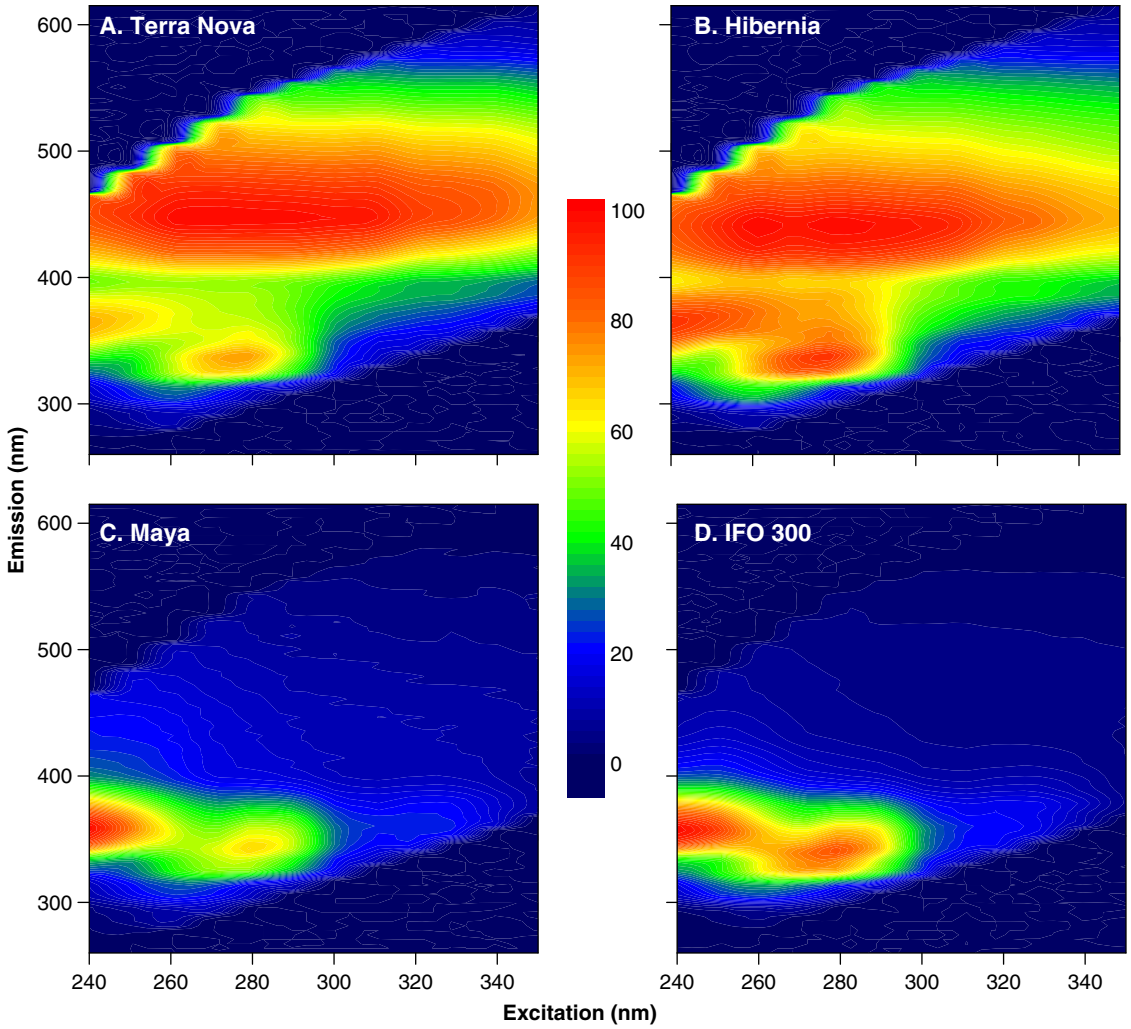


Fig. 2. Normalized intensity (reported as a percentage of maximum intensity) contour plots of excitation–emission matrix spectra (EEMs) of low viscosity (<50 cP) Terra Nova, Hibernia, and high viscosity (>50 cP) Maya, and IFO 300 crude oils.

result, the intensity data were normalized to a percentage of the maximum intensity observed. In these normalized contour plots (Figs. 1 and 2), the high intensity band observed at emission wavelengths between 320 and 360 nm (centered at approximately 340 nm) was probably associated with 1- to 3-ring aromatic structures (Wakeman, 1977). The high intensity band spanning emission wavelengths of 400–500 nm (centered at 445 nm) was probably associated with higher molecular weight ($\geqslant$3-ring) aromatics (Wakeman, 1977; Von der Dick and Kalkreuth, 1985; Smith and Sinski, 1999; Patra and Mishra, 2002). As these results are only for oil dissolved and dispersed in seawater, the absence of any emission band corresponding to the 400–500 nm band in either Maya or IFO 300 crude could be due to the low solubility of the 3-ring and larger structures (Couillard et al., 2005) and/or the dispersion of less of these fractions into the water column. It could also be a function of higher-molecular weight components that quench fluorescence non-radiatively, resulting in low fluorescence intensities (Ryder et al., 2003).

EEMS has been used to characterize or fingerprint many organic compounds in natural waters (Coble et al., 1990; Coble, 1996, with references; Stedmon et al., 2003; Sierra et al., 2006) and also to identify petroleum and oil products in particular (Von der Dick and Kalkreuth, 1985; Gugel and Siegel, 1988; Muroski et al., 1996; Booksh et al., 1996; Babichenko et al., 1999; Jiji et al., 1999; Drozdowska and Babichenko, 2002; Patra and Mishra, 2002; Nahorniak and Booksh, 2003; Christensen et al., 2005; Hegazi et al., 2005). The fingerprints of the eight test oils in Figs. 1 and 2 exhibit a number of subtle differences that could be used to identify or trace them in the environment. Of more interest is how these contour plots of the EEMs were changed when a dispersant (Corexit 9500®) was added to the oil–seawater mix.

### 4.2. Effect of dispersant on non-normalized contour plots

The EEMs in Fig. 3 summarizes the effect of the dispersant on two representative oils: Brent Blend crude (typical

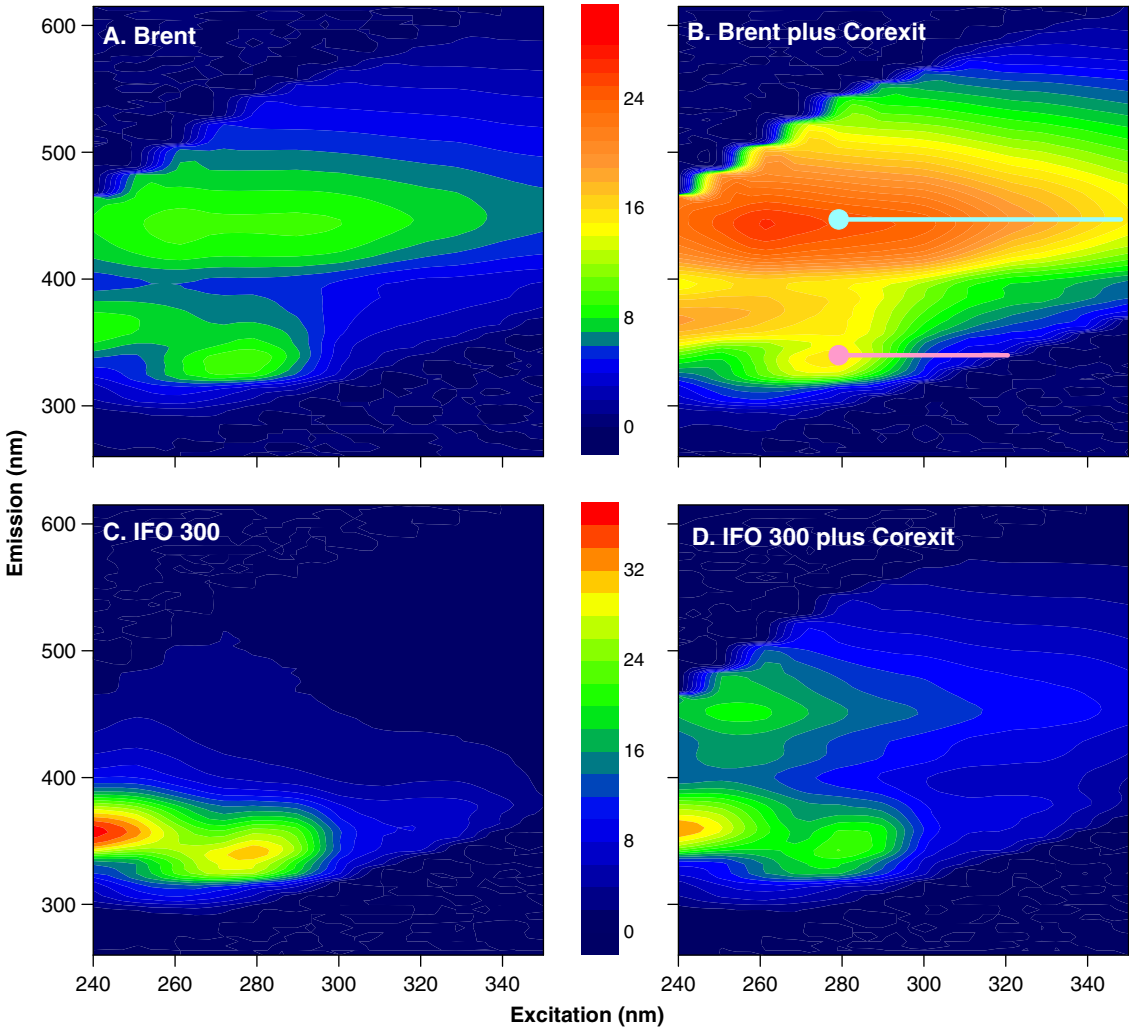


Fig. 3. Non-normalized contour plots of Brent Blend and IFO 300 crude oils dispersed in seawater and dispersed with Corexit 9500® in seawater. The pink dot indicates the position of the 340 nm-emission point at 280 nm-excitation, and the pink line delineates the excitation wavelengths over which the slope ratio was calculated. The blue dot corresponds to the 445 nm-emission at 280 nm-excitation, and the blue line delineates the excitation wavelengths over which the slope ratio was calculated.

of the test oils with DVs <50 cP) and IFO 300 (typical of the test oils with DVs >50 cP). Most noticeable in these non-normalized plots of raw fluorescence intensity is how Corexit 9500® increased fluorescence. The difference between Brent Blend (Fig. 3A) and Brent plus Corexit (Fig. 3B) is clear, with a 72% increase in intensity of the 340 nm emission band and a far larger (192%) increase in the 445 nm emission band. IFO 300 (Fig. 3C and D), displayed an even larger (530%) increase of the 445 nm band.

Yamada et al. (2003) and Couillard et al. (2005) have already shown how Corexit increases the aqueous concentrations of less water-soluble, high molecular weight PAH (>3 aromatic rings) compared to low-molecular weight PAH (with one or two rings). The increase at 445 nm can be explained by this action of the dispersant on higher-molecular weight PAH to increase its aqueous concentration by generating a larger number of smaller droplets dispersed into the water column (Lessard and Demarco, 2000; Page et al., 2000).

A more powerful analytical tool is available to quantitatively characterize EEMs. Parallel factor analysis (PARAFAC) has already been applied as a statistical tool by a number of authors to extract information from 3D plots (see e.g. Andersen and Bro, 2003, with references). It has been particularly helpful in the characterization of DOM and crude oil components in natural waters (JiJi et al., 1999; Nahorniak and Booksh, 2003; Stedmon et al., 2003; Christensen et al., 2005). Any future work should include the application of PARAFAC to multivariate studies of oil–dispersant interactions.

### 4.3. Emission ratios as a measure of the effect of dispersant

A practical method to identify and monitor chemically dispersed oil in seawater without having to measure oil concentration is needed by the oil spill response community to track the success of spill response operations. To address this issue we described the increase in fluorescence at

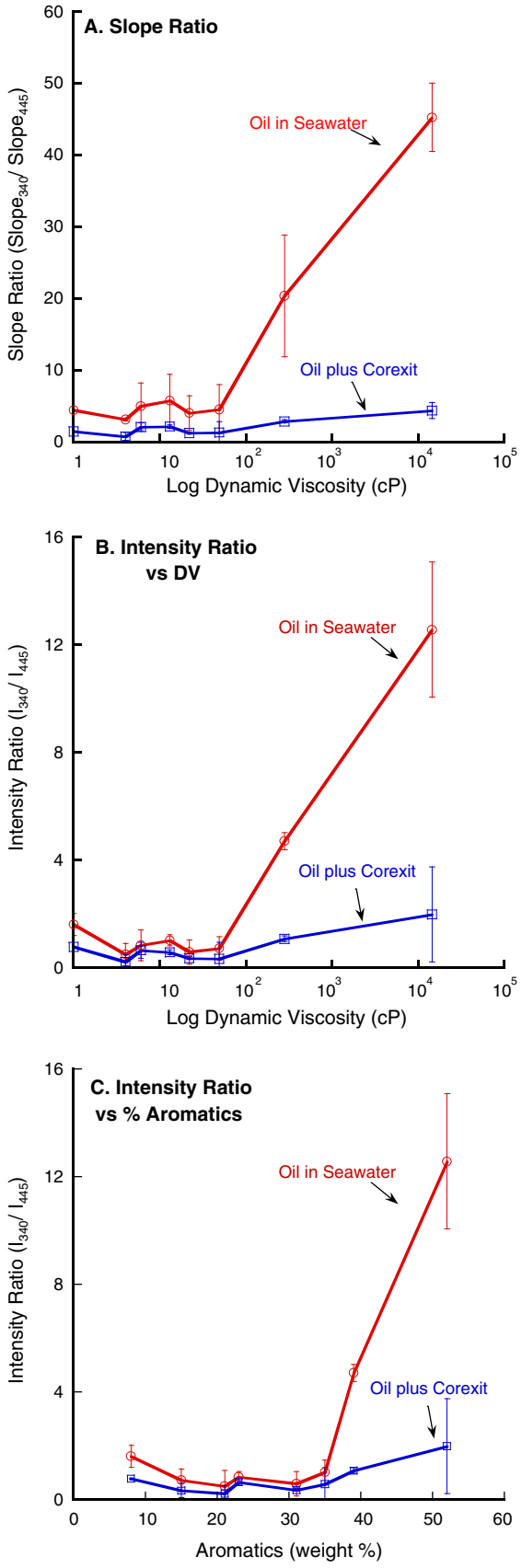


Fig. 4. Plots of the slope and intensity ratios against the log of dynamic viscosity for and weight percent aromatics of the eight test oils dispersed in seawater with and without Corexit 9500®. Bars indicate the range of values calculated from two trial runs.

445 nm in terms of a ratio calculated from emission data obtained at 340 and 445 nm. A slope ratio can be obtained from the 3D spectra by examining emission at the two wavelengths and calculating the decrease in intensity as excitation wavelengths increase. Having chosen the two principle emission bands (centered at 340 and 445 nm), we calculated the slope of emission decrease as excitation wavelength increased from 280 to 320 nm at 340 nm and from 280 to 350 nm at 445 nm (Fig. 3D). The selection of the 280 nm excitation wavelength as the starting point of slope calculations was based on it being the only excitation wavelength at which both the emission bands at 340 and 445 nm were close to an intensity maximum for all of the oils (Figs. 1 and 2). The slope at the 340 nm emission wavelength was divided by the slope at 445 nm (see e.g. Fig. 3B), and plotted for oil in seawater and oil–dispersant in seawater (Fig. 4A). Most apparent is the reduction in the slope ratio when Corexit was added. This reduction was an average of 67% for the lighter oils (with DVs <50 cP), but in excess of 85% in the case of heavier oils with DVs >50 cP (Table 2). This agrees with the EEMs in Fig. 3, where the large increase in fluorescence intensity at 445 nm is primarily responsible for reducing the slope ratio.

Taken a step further, the slope ratio can be simplified to an intensity ratio, measured as the intensity at two excitation/emission wavelength pairs – 280 nm excitation/340 nm emission and 280 nm excitation/445 nm emission. The ratios calculated from these measured values (Fig. 4B) follow a similar pattern to the slope ratios (Fig. 4A). Again, the action of dispersant was to increase the fluorescence intensity of the 445 nm emission band (Fig. 3) and drive the ratio (Fig. 4B) down to values of <2 (Table 2). This pattern was repeated when the percent aromatic content of the test oils (obtained from data supplied by Environment Canada, http://www.etc.cte.ec.gc.ca/databases/OilProperties/Default.aspx) was plotted against the intensity ratio (Fig. 4C). This could be explained by the fluorescent aromatic components of the more viscous oils becoming more dispersed as small droplets in response to Corexit 9500®, allowing them to fluoresce with more intensity at 445 nm. Even though these data suggest that there could be a simple relationship between the dispersion of aromatics and emission intensity at 445 nm, we have no direct measurements of the specific aromatic components of the test oils used in our experiments. Further analytical work is required to determine if a direct link can indeed be established between the dispersion of specific aromatics and the 445 nm emission peak.

The identification of a specific oil using either of the ratios on its own might be difficult, but the response of the ratios to dispersant is clear and consistent (Fig. 4) for the test oils that covered a range of viscosities. As a result, the effect of dispersant can be expressed as dimensionless parameters obtained from raw fluorescence data without the direct (or even indirect) measurement of oil concentration. For example, when the intensity ratios were less than a threshold value of 2 (Fig. 4), the effect of

Table 2
Values of the slope and intensity ratios for samples dispersed in seawater (SW) and dispersed in seawater with Corexit 9500® (SW + Corexit), and the percent reduction in each ratio after the addition of Corexit

| Oil | Slope ratio | | | Intensity ratio | | |
|---|---|---|---|---|---|---|
| | SW | SW + Corexit | % Reduction | SW | SW + Corexit | % Reduction |
| Scotian Light | 4.435 | 1.510 | 65.9 | 1.614 | 0.779 | 51.7 |
| Federated | 3.151 | 0.774 | 75.4 | 0.503 | 0.231 | 54.1 |
| Brent Blend | 5.006 | 2.099 | 58.1 | 0.839 | 0.654 | 22.1 |
| Gullfaks | 5.769 | 2.154 | 62.7 | 1.024 | 0.576 | 43.8 |
| Terra Nova | 4.042 | 1.256 | 68.9 | 0.594 | 0.365 | 41.8 |
| Hibernia | 4.574 | 1.334 | 70.8 | 0.724 | 0.346 | 49.6 |
| Maya | 20.352 | 2.873 | 85.9 | 4.711 | 1.086 | 76.9 |
| IFO 300 | 45.252 | 4.385 | 90.3 | 12.568 | 1.989 | 84.2 |

dispersant on the reference oils appeared to be at a maximum compared to the physical dispersion of oil alone.

Ratios could also be used to verify the action of a dispersant on a particular oil in the field. The percent reduction of the ratios after addition of Corexit to oil-in-seawater (Table 2) is an indirect estimate of the effect of chemical dispersion and was certainly enhanced (by an average of 84%) when higher-viscosity oils were treated with dispersant. Given that it is not always possible to match the response of a particular oil to a specific dispersant under a reproducible set of environmental conditions (National Research Council, 1985), the emission ratios measured here could be applied as front-line, field estimates of the efficiency of chemical oil dispersion. The ease with which a ratio can be obtained means that dispersant effectiveness can be measured under a variety of conditions during the early stages and subsequent remediation of oil spills.

At this point it should be stressed that our results have been obtained using only a single chemical dispersant, a single dispersant to oil ratio (DOR), one energy level of physical dispersion and either low- or high-viscosity, oils (with only one of intermediate viscosity). Even though there were no great differences in either the slope or intensity ratios of oils with DVs <50 cP, it is possible that the exceptionally high energy used to ensure uniform distribution of oil and oil–dispersant in seawater under laboratory conditions may have obscured subtle differences. Future work on EEMS and the dispersion process should include varying the energy of physical dispersion under standard conditions in baffled flasks (Kaku et al., 2006) and the investigation of additional oils with intermediate viscosities, along with the utilization of weathered oils and different dispersants. Even though these additional studies are required, the results of our investigations show that the application of UVFS holds promise as a means of identifying and monitoring the effectiveness of chemical oil dispersants in the field.

### 4.4. Summary

Excitation–emission spectroscopy (EEMS) has the potential to be a powerful tool for evaluating the effectiveness of chemical dispersants on oil spilled at sea. There are three reasons why EEMS is so effective:

(1) It primarily tracks the dispersion of potentially-toxic, high molecular weight fractions (with 3 or more aromatic rings) of oils in seawater (Fig. 3).
(2) Slope and intensity emission ratios calculated from the excitation–emission matrix spectra (EEMs) provide a simple, cost-effective and rapid means of detecting the efficacy of dispersants under a variety of environmental conditions.
(3) The emission ratio is also particularly useful for tracking the effect of dispersant on oils of intermediate to high dynamic viscosity (>50 cP).

The rapidity with which emission ratios can be obtained allows full EEMS, or measurements at only two emission wavelengths, to be applied as a preliminary test during an oil spill to determine if more detailed analyses are needed. In this way ultraviolet fluorescence spectroscopy (UVFS) could be employed as a front-line tool for assessing the degree of oil spill dispersion and act as a foundation for the development of remediation strategies.

## Acknowledgements

We would like to thank A.Venosa, Z. Li, and T. King and an anonymous reviewer for many useful comments on earlier versions of the manuscript. This research was supported by the Panel of Energy Research and Development (PERD) and the Department of Fisheries and Oceans, Canada.

## References

Andersen, C.M., Bro, R., 2003. Practical aspects of PARAFAC modeling of fluorescence excitation-emission data. J. Chemometrics. 17, 200–215.

Babichenko, S., Poryvkina, L., der Vos, F., Hoevenaar, H., 1999. Diagnosis of organic compounds in water quality monitoring. An application note. Int. Sci. Commun. (March), 22–24.

Biddleman, T.F., Castleberry, A.A., Foreman, W.T., Zaranski, M.T., Wall, D.W., 1990. Petroleum hydrocarbons in the surface water of two

estuaries in the southeastern United States. Estuar. Coast. Shelf Sci. 30, 91–109.

Booksh, K.S., Muroski, A.R., Myrick, M.L., 1996. Single-measurement excitation/emission matrix spectrofluorometer for determination of hydrocarbons in ocean water. 2. Calibration and quantitation of naphthalene and styrene. Anal. Chem. 68, 3539–3544.

Christensen, J.H., Hansen, A.B., Mortensen, J., Andersen, O., 2005. Characterization and matching of oil samples using fluorescence spectroscopy and parallel factor analysis. Anal. Chem. 77, 2210–2217.

Coble, P.G., 1996. Characterization of marine and terrestrial DOM in seawater using excitation–emission matrix spectroscopy. Marine Chem. 51, 325–346.

Coble, P.G., Green, S.A., Blough, N.V., Gagosian, R.B., 1990. Characterization of dissolved organic matter in the Black Sea by fluorescence spectroscopy. Nature 348, 432–435.

Couillard, C.M., Lee, K., Légaré, B., King, T., 2005. Effect of dispersant on the composition of the water-accommodated fraction of crude oil an its toxicity to larval marine fish. Environ. Toxicol. Chem. 24, 1496–1504.

Drozdowska, V., Babichenko, S., 2002. Natural water fluorescence characteristics based on LIDAR investigations of a surface water layer polluted by an oil film; the Baltic cruise – May 2000. Oceanologia 44, 339–354.

Gugel, J., Siegel, J.A., 1988. Fluorescence of petroleum products III. Three-dimensional fluorescence plots of petroleum-based products. J. Forensic Sci. 33, 1405–1414.

Hegazi, E., Hamdan, A., Mastromarino, J., 2005. Remote fingerprinting of crude oil using time-resolved fluorescence spectra. Arab. J. Sci. Eng. 30, 3–12.

JiJi, R.D., Cooper, G.A., Booksh, K., 1999. Excitation–emission matrix fluorescence based determination of carbamate pesticides and polycyclic aromatic hydrocarbons. Anal. Chim. Acta 397, 61–72.

Kaku, V.J., Boufadel, M.C., Venosa, A.D., Weaver, J., 2006. Flow dynamics in eccentrically rotating flasks used for dispersant effectiveness testing. Environ. Fluid Mech. 6, 385–406.

Keizer, P.D., Gordon Jr., D.C., 1973. Detection of trace amounts of oil in sea water by fluorescence spectroscopy. J. Fish. Res. Board Can. 30, 1039–1046.

Kepkay, P.E., Bugden, J.B.C., Lee, K., Stoffyn-Egli, P., 2002. Application of ultraviolet fluorescence spectroscopy to monitor oil–mineral aggregate formation. Spill Sci. Technol. Bull. 8, 101–108.

Lessard, R.R., Demarco, G., 2000. The significance of oil spill dispersants. Spill Sci. Technol. Bull. 6, 59–68.

Li, M., Garrett, C., 1998. The relationship between oil droplet size and upper ocean turbulence. Marine Pollut. Bull. 36, 961–970.

Muroski, A.R., Booksh, K.S., Myrick, M.L., 1996. Single-measurement excitation/emission matrix spectrofluorometer for determination of hydrocarbons in ocean water. 1. Instrumentation and background correction. Anal. Chem. 68, 3534–3538.

Nahorniak, M.L., Booksh, K.S., 2003. Optimizing the implementation of the PARAFAC method for the near-real time calibration of excitation–emission fluorescence analysis. J. Chemometr. 17, 608–617.

National Research Council, 1985. Oil in the Sea: Inputs, Fates and Effects. National Academy Press, Washington, DC, 601pp.

Østgaard, K., Jensen, A., 1983. Evaluation of direct fluorescence spectroscopy for monitoring aqueous petroleum solutions. Int. J. Environ. Anal. Chem. 14, 55–72.

Page, C.A., Bonner, J.S., Sumner, P.L., McDonald, T.J., Autenrieth, R.L., Fuller, C.B., 2000. Behaviour of a chemically-dispersed oil and a whole oil on a near-shore environment. Water Res. 34, 2507–2516.

Patra, D., Mishra, A.K., 2002. Total synchronous fluorescence scan spectra of petroleum products. Anal. Bioanal. Chem. 373, 304–309.

Ryder, A.G., Glynn, T.J., Feely, M., 2003. Influence of chemical composition on the fluorescence lifetimes of crude petroleum oils. Proc. SPIE, Int. Soc. Opt. Eng. 4876, 1188–1195.

Ryder, A.G., 2004. Assessing the maturity of crude petroleum oils using total synchronous scan spectra. J. Fluoresc. 14, 99–104.

Sierra, M.M.D., Giovanela, M., Parlanti, E., Soriano-Sierra, E.J., 2006. 3D-Fluorescence spectroscopic analysis of HPLC fractionated estuarine fulvic and humic acids. J. Braz. Chem. Soc. 17, 113–124.

Sikorska, E., Górecki, T., Khmelinski, I.V., Sikorski, M., De Keukeleire, D., 2004. Fluorescence spectroscopy for characterization and differentiation of beers. J. Inst. Brew. 110, 267–275.

Smith, G.C., Sinski, J.F., 1999. The red-shift cascade: investigations into the concentration-dependent wavelength shifts in three-dimensional fluorescence spectra of petroleum samples. Appl. Spectrosc. 53, 1459–1469.

Stedmon, C.A., Markager, S., Bro, R., 2003. Tracing dissolved organic matter in aquatic environments using a new approach to fluorescence spectroscopy. Marine Chem. 82, 239–254.

Venosa, A.D., Zhu, X., 2003. Biodegradation of crude oil contaminating marine shorelines and freshwater wetlands. Spill Sci. Technol. Bull. 8, 163–178.

Von der Dick, H., Kalkreuth, W., 1985. Synchronous excitation and three-dimensional fluorescence spectroscopy applied to organic geochemistry. Adv. Org. Geochem. 10, 633–639.

Wakeman, S.G., 1977. Synchronous fluorescence spectroscopy and its application to indigenous and petroleum-derived hydrocarbons in lacustrine sediments. Environ. Sci. Technol. 11, 272–276.

Yamada, M., Takada, H., Toyoda, K., Yoshida, A., Shibata, A., Nomura, H., Wada, M., Nishimura, M., Okamoto, K., Ohwada, K., 2003. Study on the fate of petroleum polycyclic aromatic hydrocarbons (PAHs) and the effect of chemical dispersant using an enclosed ecosystem, mesocosm. Marine Pollut. Bull. 47, 105–113.